

## STRUCTURAL AND OPTICAL PROPERTIES OF Cu-ZnO FILMS DEPOSITED BY THERMAL EVAPORATION

S. A. HUSSAIN, REHANA, B. HASSAN, N. KANWAL, S. PERVAIZ,  
M. RAZZAQ, I. A. KHAN\*

*Department of Physics, Government College University Faisalabad, 38000,  
Faisalabad, Pakistan*

Polycrystalline zinc oxide (P-ZnO) films are deposited on glass substrates for 2 min exposure time (ETs) by thermal evaporation. These P-ZnO films are further exposed in evaporated Cu species (ECuS) for different (0.5, 1, 1.5 and 2 min) ETs. XRD patterns shows the development of different planes related to ZnO phase and confirms the deposition of P-ZnO films. The shift in diffraction angle of ZnO (101) plane confirms the doping of Cu in ZnO lattice. The preferential growth orientation of P-ZnO and Cu doped ZnO films strongly depends on Cu contents and substrate surface temperature raised during deposition process. The values of crystallite size, micro-strains, dislocation density and texture coefficient of Cu doped ZnO film (deposited for 1.5 min ETs) are found to be 30.16 nm, 0.072,  $10.99 \times 10^{-4}$  nm<sup>-2</sup> and 1.66 respectively. SEM microstructure of P-ZnO film is changed with increasing ETs in ECuS. EDX analysis confirms the presence of Zn, Cu and O in the deposited films. The values of  $E_g$  of P-ZnO and Cu doped ZnO films are found to be 3.42, 2.89, 3.74, 3.65 and 2.67 eV respectively.

(Received June 4, 2019; Accepted December 4, 2019)

**Keywords:** Polycrystalline ZnO; Texture coefficient; Evaporation; Crystallite size; Energy band gap

### 1. Introduction

Zinc oxide (ZnO) is an excellent semiconductor material showing remarkable piezoelectric properties due to its hexagonal crystal structure. It has a direct wide band gap (3.37 eV) and large exciton binding energy (60 meV) at room temperature [1]. It has remarkable characteristics and natural advantages like high electronic conduction, superior luminescence and transparency at room-temperature, inexpensive, non-toxic and chemically stable. Moreover, it has found applications in several areas of interest like solar cells, UV protectors, gas sensing and photocatalysis devices [2-5]. To achieve additional properties of ZnO, it is obligatory to modify the crystal structure of ZnO by doping transition metals like Ni, Co, Al, Mn, Fe and Cu [6, 7]. Among them, Cu is exceptionally important for doping in ZnO lattice because it has high electrical conductivity and has approximately similar ionic radii. It is well known that Cu doping into ZnO lattice enhances structural, optical, physical and chemical properties of ZnO [8, 9]. Polycrystalline ZnO (P-ZnO) and Cu doped ZnO films have been deposited through various routes such as pulse laser deposition, spin coater, magnetron sputtering, chemical vapor deposition and evaporation [10-15]. However, the thermal evaporation route is more striking and valuable because it has many advantages like cost-effective, easy to maintain, environment friendly, more adhesive and better deposition rate.

In this work, the P-ZnO film and Cu-doped ZnO films are deposited on glass substrates by thermal evaporation. Five samples of P-ZnO films are deposited on glass substrates for 2 min exposure times (ETs) while the other deposition parameters like oxygen pressure (150 mtorr), source to substrate (SSD) distance (2.5 cm) and boat temperature (460 °C for Zn and 1100 °C for Cu) remains constants. The deposited P-ZnO films are further exposed to evaporated Cu species (ECuS) for different (0.5, 1, 1.5 and 2 mins) ETs. The deposited P-ZnO and Cu doped ZnO films are characterized by X-rays diffraction (XRD), scanning electron microscope (SEM) attached with

---

\*Corresponding author: ijazahmad@gcuf.edu.pk

energy dispersive X-rays (EDX) and UV spectroscopy to explore the structural, morphological and optical properties.

## 2. Experimental setup

P-ZnO and Cu doped ZnO films are deposited on glass substrates by thermal evaporation. A schematic illustration of thermal evaporation used to deposit P-ZnO and Cu doped ZnO films is shown in figure 1. The detailed information's of thermal evaporation can be found elsewhere [16-18]. Tungsten boat is connected to power supply whose current is ranged from 100-400 A. The glass substrates washed with acetone and deionized water are placed at 2.5 cm in front of tungsten boat. The zinc powder of purity 99.9 % is placed in tungsten boat connected to digital temperature meter through thermo-couple. In this work, the temperature of tungsten boat is fixed at 460°C for Zn and 1100°C for Cu powders respectively. The vacuum chamber is evacuated by rotary pump and then filled with oxygen gas of 150 mtorr pressure. The boat temperature is controlled by controlling the input current (100-400 A). The deposition process of P-ZnO and Cu doped ZnO films is divided into two steps, the deposition of (i) P-ZnO film and (ii) Cu doped ZnO films.

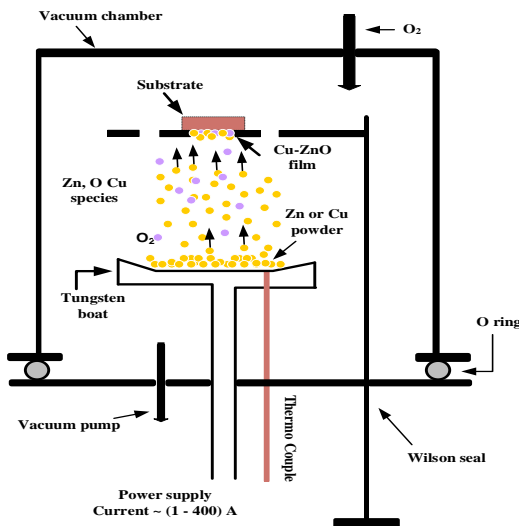
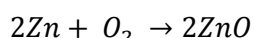


Fig. 1. Schematic diagram of thermal evaporation to deposit P-ZnO and Cu doped ZnO films.

In first step, the Zn powder placed inside the tungsten boat gets enough energy results in its evaporation. The evaporated Zn species may be in the form of atoms, molecules or ions [16-18]. The evaporated Zn species travel towards the substrate surface through oxygen environment. The reactions between the evaporated Zn and energetic O species depend on their available energy. So, the evaporated Zn and energetic O species may or may not react with each other to form ZnO phase since the evaporated Zn species are of different energies [16-18]. Both the evaporated Zn and the nucleated ZnO crystallites are condensed on the substrate surface in the form of layer. Five samples of P-ZnO films are prepared by adopting the same deposition process. The nucleation and growth of ZnO phase is governed by the following chemical equation:



Again, the Zn and ZnO crystallites may or may not arrange themselves periodically depending on their energy results in the development of amorphous or crystalline ZnO layer. In second step, the deposited P-ZnO films are further exposed to ECuS for different ETs. The Cu powder placed in tungsten boat gets enough energy results in its evaporation. The evaporated Cu species travel towards substrate surface through vacuum (no oxygen gas is present) where they

may condense as a layer on the already deposited P-ZnO film or may incorporate into Zn or ZnO lattice interstitially or substitutionally since the atomic radii of Zn and Cu are close to each other.

It is known that the evaporated Cu species reached at the substrate surface are more energetic than the evaporated Zn species because the Cu species travel through vacuum instead of oxygen environment and hence the energy losses during collisions is reduced significantly. Therefore, most probably, the energetic Cu species may incorporate into Zn or ZnO lattice instead of forming CuO phase. The energy flux of ECuS striking the substrates surface is associated with the increase of ETs. So, the total number of Cu species striking the substrate surface is increased with the increase of ETs and hence the incorporated/diffused Cu species into Zn or ZnO lattice of P-ZnO film (acts as substrate in second step) may increase with the increase of ETs. The increasing ETs of ECuS not only increase the Cu content in P-ZnO film but also increases the substrate surface temperature which play an important role to improve the film surface quality like crystal structure, surface morphology and energy band gap. We imagine that the energy of bombarded Cu species is not enough to break the strong bonding exist between Zn and O species. So, the probability of Cu species to react with oxygen is reduced and no CuO phase is formed. Therefore, the only probability for energetic Cu species striking the P-ZnO film surface, is to incorporate into Zn or ZnO lattice results in lattice distortion creating micro-strains and point defects instead of forming CuO phase.

### 3. Results and discussions

#### 3.1. Structural analysis

XRD analysis is employed to estimate the crystallite size (*C S*), micro-strains ( $\varepsilon$ ), dislocation density ( $\delta$ ), d-spacing ( $d$ ) and texture coefficient (*T C*) of ZnO (101) plane of P-ZnO and Cu doped ZnO films. A well-known relation usually called Scherer formula is employed to determine the average value of *C S* of ZnO (101) plane.

$$C S = \frac{0.9 \lambda}{FWHM \cos\theta}$$

where, 0.9 is a numerical constant (Scherer constant),  $\lambda$  is the wavelength of incident radiation,  $\theta$  is the Bragg diffraction angle and FWHM is the full width at half maxima of the diffraction plane [19-21]. The structural parameters like  $\varepsilon$ ,  $\delta$ ,  $d$  and *T C* of ZnO (101) plane are determined by employing the following relations respectively [7, 19, 22, 23].

$$\begin{aligned} \varepsilon &= \frac{FWHM \cos\theta}{4} \\ \delta &= \frac{1}{(C S)^2} \\ d &= \frac{n\lambda}{2\sin\theta} \\ T C &= N_r \frac{I_{(hkl)}/I_{o(hkl)}}{\sum I_{(hkl)}/I_{o(hkl)}} \end{aligned}$$

where  $I_{(hkl)}$  and  $I_{o(hkl)}$  are the measured and standard intensities of (*h k l*) plane respectively. Figure 2 shows the XRD patterns of P-ZnO and Cu doped ZnO films deposited for 2 and 0.5, 1, 1.5, and 2 min ETs in oxygen and ECuS environment respectively by employing thermal evaporation. XRD patterns show the development of Zn (101), Zn (100) and ZnO (101) planes appeared at  $2\theta$  values of 36.29, 38.94 and 43.17 respectively, confirming the deposition of P-ZnO

film, means the deposited P-ZnO films comprises of two (Zn and ZnO) phases. Results show that the evaporated Zn species are of two kinds corresponding to their energies the; (i) Zn species which could not react with oxygen and condense on the substrate surface showing regular arrangement of crystallites (ii) Zn species, having enough energy, react with oxygen to form ZnO phase and condense on the substrate surface showing regular arrangement of crystallites. This supports our already mentioned hypothesis that the evaporated Zn species are of various kind according to their energies. Moreover, the XRD patterns that 2 min ETs to Zn species in oxygen environment is enough to deposited P-ZnO film containing Zn and ZnO phases. It is known that the up and down shifting of diffraction plane/diffraction angle indicate the development of stresses as well as diffusion or doping of foreign element. In this case, the shift in diffraction angle of ZnO (101) pane indicates the doping of Cu species in to ZnO lattice. The P-ZnO films deposited on glass substrate for 2 min ETs in oxygen environment are so called as-deposited P-ZnO films. It is notice that the as-deposited P-ZnO film grows along Zn (101) plane preferentially while it grows preferentially along ZnO (101) plane after the doping of Cu species. When the as-deposited P-ZnO film is exposed to ECuS for 0.5 min, the bombarded Cu species delivered enough energy to the substrate surface results in the increase of substrate surface temperature which is responsible to change the crystallite arrangement and hence appearing or disappearing the diffraction planes related Zn or ZnO phase and their peak intensity and other structural parameters. The development of newly formed crystallites of ZnO (002) phase with weak intensity may be the other reason. When the as-deposited P-ZnO film is exposed to ECuS for 1 min, all the diffraction planes except ZnO (101) plane are disappeared. means the newly formed ZnO (002) phase does not remain stable for 1 min ETs in ECuS. The transformation from P-ZnO film (ZnO (101), ZnO (002)) into single crystalline ZnO film (only ZnO (101)) is accomplished with the rise in substrate surface temperature which in turn is associated with increase of ETs. When the as-deposited P-ZnO film is exposed to ECuS for 1.5 min ETs, the diffraction planes like Zn (101), Zn (100) and ZnO (101) are again developed and the peak intensity of ZnO (101) plane is maximum. It means that the Cu doped ZnO film grows preferentially along ZnO (101) plane. We have already shown that the as-deposited P-ZnO film grows preferentially along Zn (101) orientation.

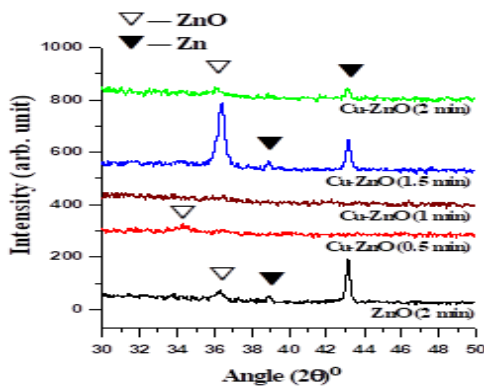


Fig. 2. XRD patterns of P-ZnO and Cu doped ZnO films.

This change in preferred orientation of Cu doped ZnO film is due to Cu doping into Zn or ZnO lattice interstitially. The rise in substrate surface temperature due to the bombardment of energetic Cu species may be the other reason. Interestingly, the intensity of all diffraction peaks is decreased when the as-deposited P-ZnO film is exposed to 2 min ETs in ECuS which is due to unfavorable rise in substrate surface temperature for larger ETs.

When the energetic ECuS are bombarded on the substrate surface, they delivered their energies to the substrate surface and causes to increase its surface temperature. It is known that the total numbers of incorporated/diffused Cu species into Zn or ZnO lattice are increased with the increase of ETs in ECuS; more the energetic Cu species striking the substrate, more energy will be delivered to the substrate surface and hence more rise in substrate surface temperature which is responsible to alter crystallites alignment and hence may improve their crystallinity.

*Table 1. Structural parameters of P-ZnO and Cu doped ZnO films with increasing ETs.*

ETs (min)	S.M.	Gas	Phases	h k l	2θ-S	2θ-O	Intensity
2	Zn	O	ZnO	101	36.25	36.29	35.99
			Zn	100	38.99	38.94	20.43
				101	43.23	43.17	163.48
Now this P-ZnO film is exposed to ECuS for various ETs							
0.5	Cu	O	ZnO	002	34.42	34.44	32.70
				101	36.25	36.29	15.09
1	Cu	O	ZnO	101	36.25	36.49	21.22
1.5	Cu	O	ZnO	101	36.25	36.39	237.56
			Zn	100	38.99	38.87	30.66
				101	43.23	43.15	114.94
2	Cu	O	ZnO	101	36.25	36.11	28.30
			Zn	100	38.99	38.83	16.51
				101	43.23	43.03	40.09

It is concluded that the improvement crystallites alignment related to Zn or ZnO phases strongly depends on the increase in substrate surface temperature which varies with the increase of ETs. It is observed that the available substrate surface temperature of Cu doped ZnO film deposited in 1.5 min ETs in ECuS is more suitable for the better its growth; having preferential growth along ZnO (101) orientation. Table 1 shows the structural parameters of P-ZnO and Cu doped ZnO films with increasing ETs. The XRD patterns show that no diffraction peak related to Cu or CuO phase is observed in Cu doped ZnO films. This shows that the ECuS travel toward the as-deposited P-ZnO film and could not react with the surface of already deposited P-ZnO film since no diffraction peak related to Cu or CuO phases are observed. However, the energetic Cu species bombarding the as-deposited P-ZnO film delivered enough energy to the surface of as-deposited P-ZnO film and hence increases the surface temperature. The amount of energy deliverance to the surface of as-deposited P-ZnO film is increased with the increase of ETs in ECuS environment. Results show that the bombarded energetic Cu species have ability to diffuse/doped into Zn or ZnO lattices, however, the doping contents is increased with the increase of ETs in ECuS environment. The doping content of Cu species into Zn or ZnO lattices is increased with the increase of ETs in ECuS environment. The doping of Cu content into Zn or ZnO lattice is also confirmed from the up and down shifting of diffraction angle. The development of no diffraction peak related to Cu or CuO phase shows that (i) Cu species could not aligned themselves in regular pattern and (ii) Cu could not react with the already present oxygen at the surface of as-deposited P-ZnO film. Moreover, the bombarded Cu species could not deliver enough energy to break the Zn-O bond and hence no CuO phase is formed. It means that the energy delivered to substrate surface is smaller than the activation energy required to break the Zn-O bond. While the EDX analysis (discuss later) reveals the presence of Cu species in the Cu doped ZnO films. It means that Cu species are doped into Zn or ZnO lattice instead of forming crystalline Cu or CuO phases and how much doing of cu is there, it depends on the energy of the incorporated species. It has been pointed out that the Cu species were incorporated into Zn or ZnO lattice interstitially or substitutionally because Cu can replace either substitutionally or interstitially by Zn atoms in ZnO lattice leading to structural deformations [24, 25].

Fig. 3 illustrates the change in diffraction angle of ZnO (101) plane with increasing ETs in ECuS. A small up shift in ZnO (101) plane indicates the presence of compressive stresses because the up and down shifting of any diffraction plane shows the presence of compressive and tensile stresses respectively [26, 27]. This up shifting of ZnO (101) plane is further increased with the increase of ETs (up to 1 min) in ECuS; due to the incorporation of Cu content in ZnO lattice interstitially. The up shifting of ZnO (101) plane is decreased with the further increase of ETs (1.5

min) results in the decrease of compressive stresses. This decrease in compressive stresses is responsible to increase the crystallinity of ZnO film. A down shift in ZnO (101) plane is observed with the further increase of ETs (2 min) which indicates the presence of tensile stress.

Such type of stress transformation (from compressive to tensile) was observed in ZrN films due to the incorporation of impurity or one of the involved species interstitially into the lattice of other phase. The presence of stresses and their transformation are also responsible to improve the mechanical properties like hardness [26, 27]. Figure 4 reveals the variation of average C S and peak intensity of ZnO (101) plane of P-ZnO and Cu doped ZnO films with increasing ETs. The average C S and peak intensity of ZnO (101) plane are increased up to 1.5 min ETs and then start to decrease with the further increase of ETs. The values of these structural parameters are maximum for 1.5 min ETs showing improved crystallinity which is due to stress relaxation effect and corresponding substrate surface temperature.

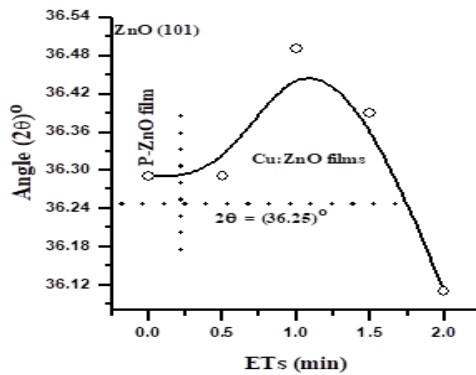


Fig. 3. Change in diffraction angle of ZnO (101) plane with increasing ETs.

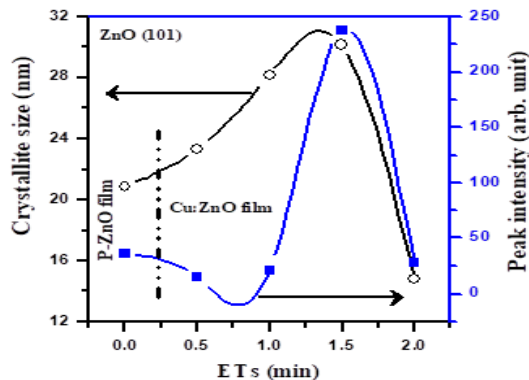


Fig. 4. Variation of average C S and peak intensity of ZnO (101) plane with increasing ETs.

Fig. 5 shows the variation of micro-strains and dislocation density developed in ZnO (101) plane of the as-deposited P-ZnO and Cu doped ZnO films with increasing ETs. A similar trend in the variation of these parameters with increasing ETs is observed. It is known that the doping of Cu contents into Zn or ZnO lattices is associated with the increase of ETs. It is concluded that there is a direct relation between the C S and peak intensity and dislocation density and micro-strains developed in the as-deposited ZnO and Cu doped ZnO films. It is obvious that smaller the values of micro-strains and dislocation density; higher will be the C S and peak intensity of the deposited films.

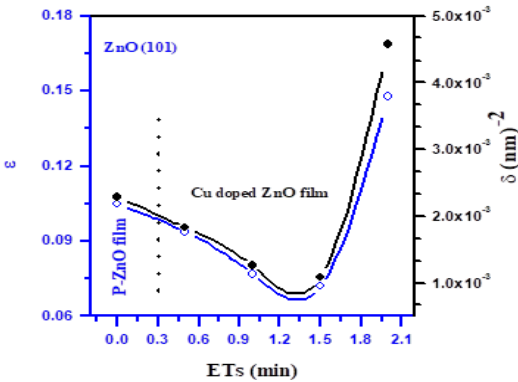


Fig. 5. Variation of  $\varepsilon$  and  $\delta$  developed in ZnO (101) plane of P-ZnO and Cu doped ZnO films.

The values of  $T C$  of ZnO (101), Zn (101) and Zn (100) planes of P-ZnO film are found to be 0.43, 1.96 and 0.61 respectively. The values of  $T C$  of ZnO (101), Zn (101) and Zn (100) planes in Cu doped ZnO film (for 1.5 min ETs) are found to be 1.66, 0.80 and 0.54 respectively. The values of  $T C$  of Zn (101) plane for as-deposited P-ZnO and ZnO (101) plane for Cu doped ZnO films (deposited for 1.5 min ETs) are maximum and more than one respectively. The as-deposited P-ZnO grows preferentially along Zn (101) orientation while the Cu doped ZnO film grows preferentially along ZnO (101) respectively. It means the doping of Cu contents into Zn or ZnO lattice is responsible to change the preferred orientation along with the film surface quality.

### 3.2. SEM analysis

The surface morphology of P-ZnO and Cu doped ZnO films deposited on glass substrates is investigated by SEM analysis. Figure 6 demonstrates the SEM microstructures of P-ZnO and Cu doped ZnO films prepared in oxygen environment for 2 min and in ECuS for 0.5, 1, 1.5, 2 min ETs respectively.

The surface morphology of P-ZnO film has irregular elongated narrow paths forming complicated microstructures. Few larger rounded particles are embedded in the irregular elongated narrow paths of P-ZnO film which makes the surface rough. When the P-ZnO film is exposed in ECuS for 0.5 min ETs, amazingly, the larger particles are decomposed into relatively smaller rounded particles showing uniform distribution. The Cu doped ZnO film is free from the irregular elongated narrow paths and cracks. The decomposition of larger rounded particles and the re-structuring of the irregular elongated narrow paths into smaller rounded particles is because of Cu doping into Zn or ZnO lattice interstitially (XRD analysis). The rise in substrate surface temperature during the bombardment of energetic Cu species may be the other reason to decompose the larger rounded particles and re-structuring of narrow paths. The relatively few larger rounded particles are also observed which contains smaller rounded particles. The larger rounded particles and their agglomerates are further decomposed into smaller rounded particles when the P-ZnO film is exposed for 1 min in energetic ECuS showing approximately same shape and sizes and are distributed uniformly.

The larger agglomerates comprising of smaller rounded particles are isolated through their grain boundaries which hinders the slip motions and hence enhances the mechanical properties. The isolation of rounded particles through their grain's boundaries and the hindering of slip motions may also influence on the optical properties like energy band gap and absorption coefficient. The size of agglomerated round particles increases significantly and gives rise to one huge rounded particle when the P-ZnO film is exposed to 2 min in ECuS environment. Moreover, such type of surface morphologies having uniform distribution of particles and their agglomerates are observed in Cu doped ZnO films [25]. It is concluded that the surface morphology of P-ZnO films depends on the diffused Cu contents in to Zn or ZnO lattice which is increased with the increase of ETs. The rise in substrate surface temperature of Cu doped ZnO films may be the other reason to change the micro-structural features of Cu doped ZnO films. The decomposition of

larger rounded particles to smaller one along with the formation of agglomerates and their growth with increasing ETs may influence the film surface properties.

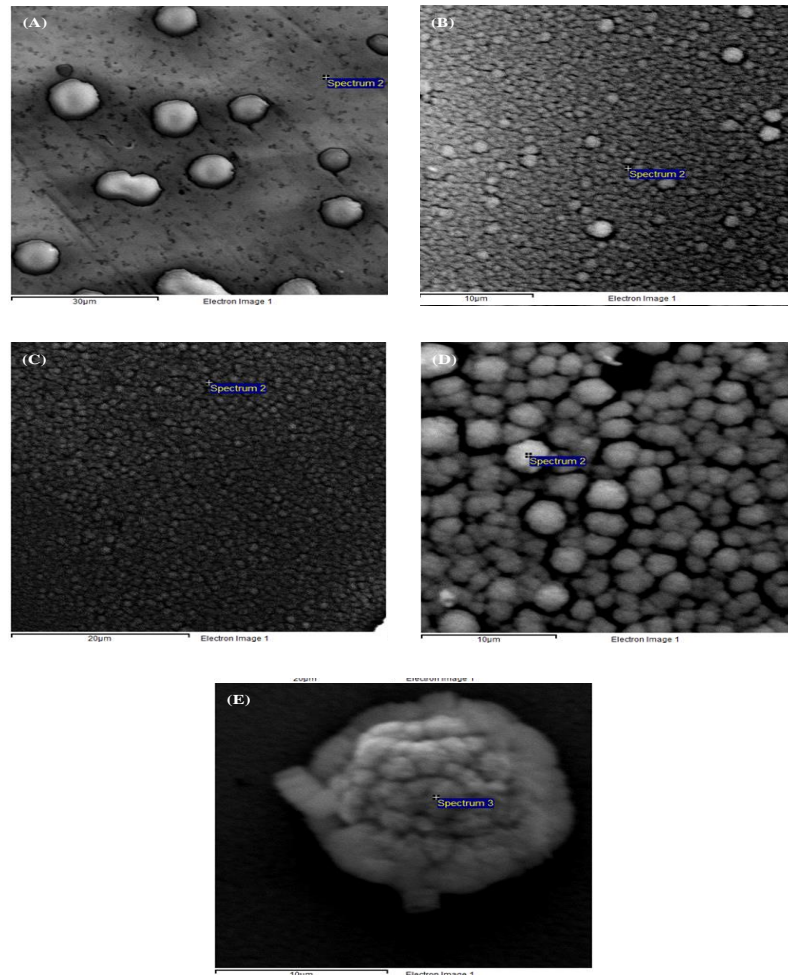


*Fig. 6. SEM microstructures of P-ZnO film deposited for (A) 2 min in oxygen and Cu doped. ZnO films deposited for (B) 0.5; (C) 1; (D) 1.5 and (E) 2 min ETs in ECuS environment respectively.*

### 3.3. EDX analysis

The quantitative analysis of P-ZnO and Cu doped ZnO films is investigated by EDX analysis. Fig. 7<sub>A-B</sub> reveals the typical EDX spectra of P-ZnO (deposited for 2 min ETs in oxygen environment) and Cu doped ZnO film (deposited for 1.5 min ETs in ECuS environment). The peaks related to Zn, O and Cu elements confirms their presence in the deposited P-ZnO and Cu doped ZnO films. The other peaks in EDX spectra are related to glass substrate. Table 2 shows the variation of Zn, O and Cu contents in P-ZnO and Cu doped ZnO films with increasing ETs.

Table 2. Variation of Zn, O, and Cu contents in P-ZnO and Cu doped ZnO films deposited in oxygen and ECuS environment for different ETs.

ETs (min)	Source material	Working gas	Phases	Elemental composition (at. %)		
				Zn	O	Cu
2	Zn	Oxygen	ZnO	26.09	39.17	-----
Five P-ZnO films are deposited on glass substrates, four P-ZnO films are further exposed in ECuS to form Cu doped ZnO films, according to the following parameters						
0.5	Cu	Oxygen	Cu: ZnO	18.57	42.53	9.69
1	Cu	Oxygen	Cu: ZnO	14.42	43.15	10.91
1.5	Cu	Oxygen	Cu: ZnO	11.61	44.83	11.18
2	Cu	Oxygen	Cu: ZnO	9.16	49.22	12.44

The Zn, O and Cu contents in P-ZnO film deposited for 2min ETs are found to be 26.09, 39.17 and 0 at. % respectively. The Zn, O and Cu contents in Cu doped ZnO film deposited in ECuS environment for 1.5 min ETs are found to be 11.61, 44.83 and 11.18 at. % respectively. The Zn content is decreased gradually while O and Cu contents are increased in Cu doped ZnO films with increasing ETs. This decreasing Zn and increasing Cu and O contents indicates the increase of film thickness with increasing ETs. A slight increase in O content in Cu doped ZnO films is due to the formation of native oxides which are produced during the deposition process of Cu doped ZnO films at high temperature. These native oxides are of smaller energy, could not react with evaporated Cu species (XRD results) as no diffraction peak related to Cu or CuO phase is observed. It is concluded that the change in elemental composition in Cu doped ZnO films play an important role to change the film surface properties such as structural, morphological and optical properties.

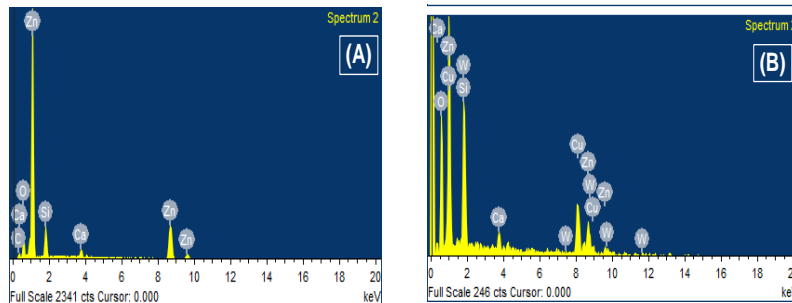


Fig. 7 EDX spectra of: (A) P-ZnO deposited for 2 min in oxygen and (B) Cu doped ZnO films deposited for 1.5 min ETs in ECuS environment respectively.

### 3.4. Optical analysis

The optical characterization of thin films provides the information about the optical parameters like absorption coefficient ( $\alpha$ ) and energy band ( $E_g$ ) gap. The absorption spectra are used to calculate the  $\alpha$  and  $E_g$  of P-ZnO and Cu doped ZnO films. The  $\alpha$  is determined by employing the following formula [28].

$$\alpha = \frac{2.303 A}{d}$$

where  $A$  and  $d$  are the absorbance and film thickness. The thickness of P-ZnO and Cu doped ZnO films deposited for various ETs is ranged from 800 to 1000 nm.

The values of optical band gap of P-ZnO and Cu doped ZnO films are calculated by employing the following relation (commonly known as Tauc's plot) [29-31].

$$\alpha h\nu = B(h\nu - E)^n$$

where  $h\nu$  and  $B$  are the photon energy and constant respectively. The constant  $B$  does not depend on  $h\nu$ . It is known that the exponent  $n$  varies from material to material. For direct band gap semiconducting material, the value of exponent is equal to 0.5 or 0.67, however, 0.5 is more suitable for ZnO film because it gives a linear plot between  $\alpha$  and  $h\nu$ .

Figure 8 exhibits the absorption spectra of P-ZnO and Cu doped ZnO films deposited for different ETs. The absorption edge of P-ZnO and Cu doped ZnO films are in the wavelength ranged from 292 to 302 nm for P-ZnO film because it is a direct band gap semiconducting material.

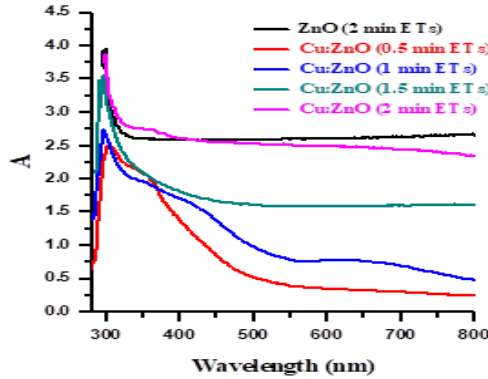


Fig. 8. Absorption spectra of P-ZnO and Cu doped ZnO films deposited for different ETs.

A strong absorption occurs in the wavelength ranged from 292 nm to 363 nm whereas a weak absorption is observed for the wavelength ranged from 400 nm to 800 nm comparatively. The absorption of P-ZnO film in the wavelength ranged from 400 to 800 is maximum which is decreased significantly for 0.5 min ETs and then starts to increase with the further increase of ETs. Table 2 shows that Cu (9.69 at. %) in ZnO lattice is responsible to decrease the absorption in higher wavelength range, however, the absorption is increased significantly with the further increase of Cu content (10.91-12.44 at. %) in Cu doped ZnO films. The change in doping content is responsible to change the absorption of Cu doped ZnO films. Moreover, the change in absorption of P-ZnO and Cu doped ZnO films may be due to the nature of deposited films (amorphous or crystalline), preferred orientation, stress transformation, T C and C S. This change in structural parameters may fluctuate the  $\alpha$  and  $E_g$  of P-ZnO and Cu doped ZnO films.

Fig. 9 represents the Tauc's plot between the photon energy of P-ZnO and Cu doped ZnO films deposited in oxygen and ECuS for different ETs respectively. The value of  $E_g$  of P-ZnO film is found to be  $\sim 3.42$  eV which is close to the literature value [1]. The value of  $E_g$  of Cu doped ZnO film treated for 0.5 min ETs in ECuS decreases to 2.89 eV which is due to the structural change like change in peak intensity and the development of new plane. The value of  $E_g$  of single crystalline Cu doped ZnO film (treated for 1 min ETs in ECuS) is further decreased to 2.67 eV which is due to the weak intensity of ZnO (101) plane and non-stability ZnO (002) plane. The  $E_g$  of Cu doped ZnO film treated for 1.5 min ETs in ECuS is maximum (3.74 eV) which is due to the maximum crystallinity of ZnO (101) plane and the change in preferred orientation.

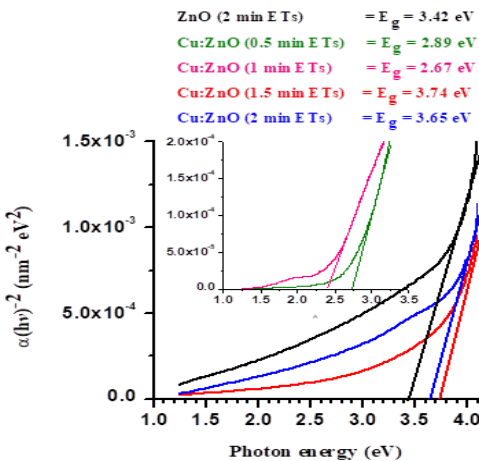


Fig. 9. Variation of  $E_g$  of P-ZnO and Cu doped ZnO films deposited for various ETs.

The maximum values of T C (1.66) and C S (30.16 nm) of ZnO (101) plane may be the other reasons. The value of  $E_g$  of Cu doped ZnO film treated for 2 min in ECuS is again decreased to 3.65 eV which is due to the stress transformation (from compressive to tensile) and weak peak intensities. Joshi et al [25] have reported that the energy band gap widening and narrowing of Cu doped ZnO films depend on the variation of Cu contents and residual stresses. The values of  $E_g$  of Cu doped ZnO films may decrease or increase up to approximately 1 eV depending on Cu content and micro-defects. In our case, the widening and narrowing of  $E_g$  of the as-deposited Cu doped ZnO films is due to the change in Cu contents, crystalline nature (single crystal or polycrystalline), C S, T C and stress transformation.

The maximum value of  $E_g$  is found to be 3.74 eV of Cu doped ZnO film treated for 1.5 min ETs in ECuS which is due to maximum crystallinity (237.56), C S (30.16 nm) and T C of ZnO (101) plane. The  $E_g$  of Cu doped ZnO film is decreased to 3.64 eV when P-ZnO film is treated for 2 min in ECuS which is due to weak crystallinity, stress transformation, relatively higher values of  $\epsilon$  and  $\delta$ . This shows that weak crystallinity, C S, stresses transformation and defects like  $\epsilon$  and  $\delta$  are responsible to decrease the  $E_g$  of Cu doped ZnO film. It is concluded that the  $E_g$  widening and narrowing of Cu doped ZnO films is due to the change of film nature because the values of  $E_g$  are decreased when the nature of deposited film is change from good polycrystalline to weak polycrystalline and to single crystalline.

#### 4. Conclusions

P-ZnO and Cu doped ZnO films are deposited on glass substrates by thermal evaporation. XRD patterns reveals the formation of P-ZnO, single and polycrystalline Cu doped ZnO films. The stress transformation in P-ZnO and Cu doped ZnO films depends on the increasing ETs. The values of crystallite size, micro-strains, dislocation density and texture coefficient of Cu doped ZnO film (deposited for 1.5 min ETs) are found to be 30.16 nm, 0.072,  $10.99 \times 10^{-4} \text{ nm}^{-2}$  and 1.66 respectively. The formation of single and polycrystalline P-ZnO and Cu doped ZnO films is attributed to increasing ETs, Cu content and substrate surface temperature raised during deposition process. FESEM analysis reveals the formation of nano-particles of various shapes, sizes and distribution and the change in all these microstructural features are associated with the increase of ETs in ECuS. EDX analysis confirms the presence of Zn, Cu and O in the deposited P-ZnO and Cu doped ZnO films, however the contents of these elements are change with increasing ETs.

The values of  $E_g$  of P-ZnO and Cu doped ZnO films are found to be 3.42, 2.89, 3.74, 3.65 and 2.67 eV respectively. The values of  $E_g$  of Cu doped ZnO film can be decreased or increased up to  $\sim 1$  eV and it only depends on the variation of structural parameters like nature of the deposited

film (amorphous, single and poly crystalline), crystallinity, C S, T C, residual stresses, stress transformation and the formation of agglomerates.

### **Disclosure statement**

No potential conflict of interest was reported by the authors.

### **Acknowledgement**

The authors would like to thank the Higher Education Commission, Pakistan for proving funds to install thermal evaporator at Thin Films Deposition Lab, Department of Physics, GC University Faisalabad.

### **References**

- [1] C. F. Klingshirn, A. Waag, A. Hoffmann, J. Geurts, Springer (2010).
- [2] F. Xu, P. Zhang, A. Navrotsky, Z-Y. Yuan, T-Z Ren, M. Halasa, B-L Su, *Chem. Mater.* **19**, 5680 (2007).
- [3] A. B. F. Martinson, J. W. Elam, J. T. Hupp, M. J. Pellin, *Nano Lett.* **7**, 2183 (2007).
- [4] R. H. Wang, J. H. Xin, X. M. Tao, *Inorg. Chem.* **44**, 3926 (2005).
- [5] M. Yang , D. Wang , L. Peng, T. Xie, Y. Zhao, *Nanotechnology* **17**, 4567 (2006).
- [6] D. Bresser, F. Mueller, M. Fiedler, S. Krueger, R. Kloepsch, D. Baither, M. Winter, E. Paillard, S. Passerini, *Chem. Mater.* **25**, 4977 (2013).
- [7] K. D. A. Kumar, V. Ganesh, S. Valanarasu, M. Shkir, I. Kulandaismayy, A. Kathalingam, S. AlFaify, *Mater. Chem. Phys.* **212**, 167 (2018).
- [8] M. Sajjad, I. Ullah, M. I. Khan, J. Khan, M. Y. Khan, M. T. Qureshi, *Results in Physics* **9**, 1301 (2018).
- [9] B. Allabergenov, S-H. Chung, S. M. Jeong, S. Kim, B. Choi, *Optical Materials Express* **3**, 1733 (2013).
- [10] D. J. Cohen, K. C. Ruthe, S. A. Barnett, *Journal of Applied Physics* **96**, 459 (2004).
- [11] S-S. Lin, J-L. Huang, P. Šajgalik, *Surf. Coat. Technol.* **185**, 254 (2004).
- [12] A. Martín, J. P. Espinós, A. Justo, J. P. Holgado, F. Yubero, A. R. González-Elipe, *Surf. Coat. Technol.* **151/152**, 289 (2002).
- [13] J. Mass, P. Bhattacharya, R. S. Katiyar, *Mater. Sci. Eng. B* **103**, 9 (2003).
- [14] H. Kim C. M. Gilmore, J. S. Horwitz, A. Piqué, H. Murata, G. P. Kushto, R. Schlaf, Z. H. Kafafi, D. B. Chrisey, *Appl. Phys. Lett.* **76**, 259 (2000).
- [15] M. Kumar, R. M. Mehra, A. Wakahara, M. Ishida, A. Yoshida, *J. of Appl. Phys.* **93**, 3837 (2003).
- [16] I. A. Khan, M. Noor, A. Rehman, A. Farid, M. A. K. Shahid, M. Shafiq, *Eur. Phys. J. Appl. Phys.* **72**, 30302 (2015).
- [17] I. A. Khan, M. Noor, A. Rehman, N. Kanwal, A. Farid, S. Z. Bajwa, W. S. Khan, M. A. K. Shahid, M. Shafiq, *J. of Optoelect. Adv. Mater.* **18**, 322 (2016).
- [18] I. A. Khan, N. Amna, N. Kanwal, M. Razzaq, A. Farid, N. Amin, U. Ikhlaq, M. Saleem, R. Ahmad, *Mater. Res. Express* **4**, 036402 (2017).
- [19] B. D. Cullity, S. R. Stock, *Elements of X-ray Diffraction*, Prentice Hall, New Jersey (2001).
- [20] G. K. Williamson, R. E. Smallman, *J. Phil. Mag.* **1**, 34 (1956).
- [21] X. S. Wang, Z. C. Wu, J. F. Webb, Z. G. Liu, *Appl. Phys. A* **77**, 561 (2003).
- [22] Z. R. Khan, M. Zulfequar, M. S. Khan, *Mat. Sci. Eng. B* **174**, 145 (2010).
- [23] Z. R. Khan, M. S. Khan, M. Zulfequar, *Mat. Sci. Appl.* **2**, 340 (2011).
- [24] K. Yamamoto, K. Nagasawa, T. Ohmori, *Physica E* **24**, 129 (2004).

- [25] K. Joshi, M. Rawat, S. K. Gautam, R. G. Singh, R.C. Ramola, F. Singh, J. of Alloy. Comp. **680**, 252 (2016).
- [26] L. Bertalot, H. Herold, U. Jäger, A. Mozer, T. Oppenländer, M. Sadowski, H. Schmidt, Physics Letters A **79**, 389 (1980).
- [27] I. A. Khan, R. S. Rawat, R. Ahmad, M. A. K. Shahid, Appl. Surf. Sci. **288**, 304 (2014).
- [28] K. B. Kumar, P. Raji, Rec. Res. Sci. Technol. **3**, 48 (2011).
- [29] J. Szczyrbowski, A. Dietrich, H. Hoffmann, Phys. Status Solidi. **78**, 243 (1983).
- [30] N. Nithya, S. R. Radhakrishnan, Advance Appl. Sci. **3**, 4041 (2012)
- [31] S. S. Shariffudin, M. Salina, S. H. Herman, M. R. Mahmood, Transactions on Electrical and Electronic Materials **13**, 102 (2012).